Coherent Structures in Localized and Global Pipe Turbulence

Ashley P. Willis* and Rich R. Kerswell†

Department of Mathematics, University of Bristol, University Walk, Bristol BS8 1TW, United Kingdom

(Received 19 June 2007; published 24 March 2008)

The recent discovery of unstable traveling waves (TWs) in pipe flow has been hailed as a significant breakthrough with the hope that they populate the turbulent attractor. We confirm the existence of coherent states with internal fast and slow streaks commensurate in both structure and energy with known TWs using numerical simulations in a long pipe. These only occur, however, within less energetic regions of (localized) ''puff'' turbulence at low Reynolds numbers (Re = 2000–2400), and not at all in (homogeneous) ''slug'' turbulence at Re = 2800. This strongly suggests that all currently known TWs sit in an intermediate region of phase space between the laminar and turbulent states rather than being embedded within the turbulent attractor itself. New coherent fast streak states with strongly decelerated cores appear to populate the turbulent attractor instead.

DOI: 10.1103/PhysRevLett.100.124501 PACS numbers: 47.27.Cn, 47.20.Ft, 47.60.−i

The transition to turbulence in wall-bounded shear flows is a classical problem that has challenged physicists for over a century. Some flows, such as that between differentially heated parallel plates or between rotating concentric cylinders, exhibit a smooth progression to increasingly complicated flows via an initial linear instability. Plane Couette flow and pipe flow, however, abruptly adopt a turbulent state. The problem is further complicated by changes in the spatiotemporal character of the observed flows at different flow rates. Pipe flow exhibits a quasistable localized turbulent ''puff'' state as well as a globally turbulent ''slug'' flow [1]. A finite amplitude disturbance is required to trigger turbulence, the amplitude of which has been shown to depend critically on its ''shape'' [2]. Similarly, plane Couette flow exhibits localized spots of turbulence which may be either short lived transients or survive to arbitrarily long times [3]. Plane Poiseuille flow, on the other hand, exhibits a linear instability but at flow rates well beyond those at which turbulence is typically observed.

The discovery of exact traveling wave (TW) solutions in wall-bounded shear flows [4–9] has spurred a flurry of excitement within the community and prompted the speculation that the states lie inside the turbulent attractor. As TWs appear only to have a few unstable directions in phase space [7,10], a turbulent flow trajectory is imagined to wander between these states, with the probability of the flow ''visiting'' a particular TW determined by how unstable it is. The hope is that turbulent statistics are then predictable from an appropriately-weighted sum of all the relevant TW properties (see the reviews [11,12]).

Pipe flow has emerged as the main setting to confirm this picture. Thus far, numerical results have been confined to unrealistically short periodic pipes [10,13], and while experimental observations suggest evidence of TWs, important structural differences remain [compare Figs. (2e),(2f), 4 in [14] and Fig. 1 in [15]). In this Letter, we use direct numerical simulations in a sufficiently long pipe to capture real localized (puff) and global (slug) turbulent states, in order to determine whether TWs populate the turbulent attractor. The ability to accurately simulate spatially inhomogeneous turbulence at transitional Reynolds numbers proves crucial in revealing the true position of the TWs in phase space.

The nondimensionalized governing Navier-Stokes equations for an incompressible fluid are

$$\partial_t \boldsymbol{u} + \boldsymbol{u}\cdot\boldsymbol{\nabla}\boldsymbol{u} + \boldsymbol{\nabla} p = \frac{1}{\mathrm{Re}}\nabla^2\boldsymbol{u}, \qquad \nabla\cdot\boldsymbol{u} = 0, \tag{1}$$

where the Reynolds number $\mathrm{Re} := UD/\nu$ (U is the mean axial flow speed, D is the pipe diameter and ν is the fluid's kinematic viscosity). These are solved in a pipe of length $50D$ across which periodic boundary conditions are imposed at constant Re (mass flux) in cylindrical coordinates (r, θ, z) using the formulation and numerical resolution described in [16]. (At Re = 2800, the energy of spectral coefficients falls by at least 6 orders of magnitude with spectral order in either r, θ or z).

Data were collated from simulations over a range of Re up to 3500 and over times of greater than $3000D/U$; the skin friction is a useful indicator of the flow response—see Fig. 1. A localized puff structure [1] of apparently stable length $\approx 20D$ is observed for $\mathrm{Re} \lesssim 2250$. At $2250 \lesssim \mathrm{Re} \lesssim 2500$ the puff gradually expands while translating along the pipe, possibly dividing into multiple puffs, giving rise to an uneven patch of turbulence in which the turbulent intensity is spatially inhomogeneous [see Figs. 2(a)–2(c)]. By $\mathrm{Re} \approx 2800$, the turbulent intensity has become much more spatially homogenized indicating slug-like turbulence [1].

As a puff is spatially inhomogeneous, the search for coherent structures was conducted at fixed relative positions, up- and downstream, of the puff's steadily translating trailing edge, $z_{\mathrm{TE}}(t)$, which is itself characterized by a sharp jump in the streamwise velocity u_z on the pipe axis [17]. The search focused upon the appearance of fast streaks near the pipe wall; thus, correlations in the stream-

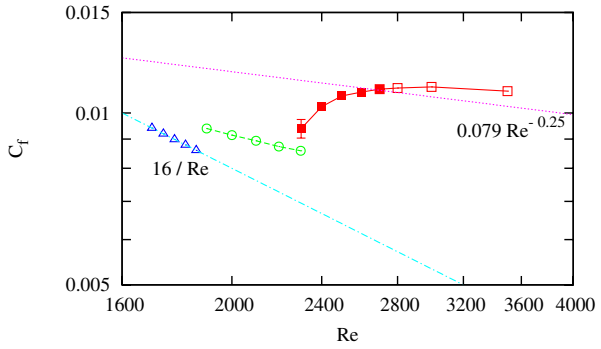

FIG. 1 (color online). Skin friction coefficient $C_f = -\langle \partial_z p \rangle_{r\theta zt} D/2\rho U^2$ for a $50D$ pipe where ρ is the fluid density. Triangles—laminar flow; circles—puffs; solid squares—spatially inhomogeneous turbulence and open squares—homogeneous slug turbulence (the transition is gradual). The lower straight line corresponds to laminar flow and the upper to the Blasius friction law which is initially overshot by the turbulent flow [23]. At Re = 2300 the flow alternates between a 1 puff state (circle) and 2 or 3 puff states (square with error bars).

wise velocity were examined using the function

$$C(\theta, z') = \frac{2\langle u_z'(\theta + \phi, z') u_z'(\phi, z') \rangle_\phi}{\langle \max_{\phi,z} (u_z')^2 \rangle_t} \Bigg|_{r=0.4D}, \quad (2)$$

where $\langle \cdot \rangle_s$ indicates averaging over the subscripted variable, and u_z' is the deviation from the time-averaged profile calculated for each $z' = z - z_{\mathrm{TE}}$ position in the puff. The projection function $C_m(z') = 2\langle C(\theta, z') \cos(m\theta) \rangle_\theta$ was used to extract the signature of structures of azimuthal wave number m. Experience of examining flow structures indicated that a "good" correlation is achieved for $C_m(z')$ larger than 0.1, as indicated by Fig. 3, which shows the correlation results for the puff snapshot of Fig. 2(c). The magnitude of the correlation measures are relatively large at the positions indicated in Fig. 3 despite not being located at z_{TE}, where the turbulent intensity is greatest (u_z' is largest) for the puff. Cross sections in (r, θ) of the flow field are shown in Fig. 2(d) with lines indicating their position. For comparison purposes, cross-sections for another puff snapshot are reproduced in Fig. 2(e) where $C_m(z')$ is less than 0.1 for all z'. Particularly for the plots upstream of the trailing edge, the similarity to known TWs is remarkable where individual slow streaks are also reproduced in the interior (compare, for example, with Figs. 9a and 13 (lower left) in [8]).

The probabilities of finding a correlation greater than 0.1 at different parts of the puff are plotted in Fig. 4. From around $z' = -D$ to $z' = +5D$ fast streak structures of $m = 3$ and $m = 4$ are seen approximately 10%–15% of the time which is in good agreement with the frequencies observed in [10,13,18]. The appearance of coherent fast streaks, however, does not necessarily imply an observation of a TW. Of the coherent fast streak structures found, those which look most like TWs (in terms of fast *and* slow streaks) are found away from the most energetic regions in puff turbulence. The disturbance energy at the trailing edge itself (Fig. 5) is far too high to be compatible with any known TW at the same Re with the roll energy, in particular, an order of magnitude too large. Cross sections at z_{TE} also exhibit small-scale structure uncharacteristic of TWs [see Fig. 2(g)]. Upstream and downstream, at approximately $z' = -2D$ and $z' = +4D$, where we find well

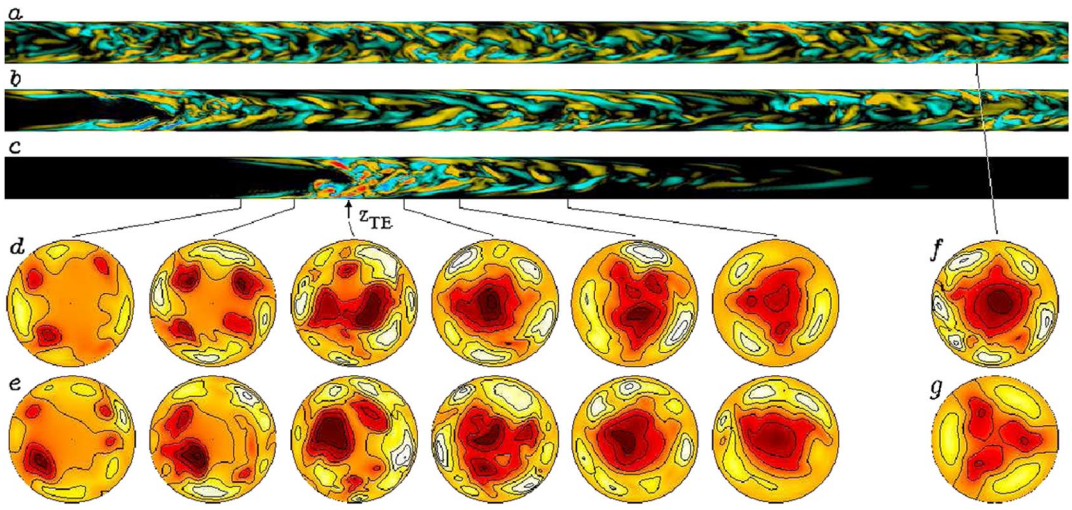

FIG. 2 (color online). Axial component of vorticity in (r, z)-plane, $25D$ shown of $50D$ computational domain; (a) slug turbulence at Re = 2800; (b) inhomogeneous turbulence at Re = 2400 (c) puff turbulence at Re = 2000. Cross sections in (r, θ) show the axial flow relative to the laminar profile with fast streaks (light/white) and slow streaks (dark/red), contour lines each $0.2U$; (d) $m = 4$ and $m = 3$ structures seen upstream and downstream of the trailing edge z_{TE} (flow is left to right); (e) sections from a puff where no clear structures are observed; (f) energetic section at Re = 2800, but resembling $m = 5$ structure; (g) exact solution with threefold rotational symmetry.

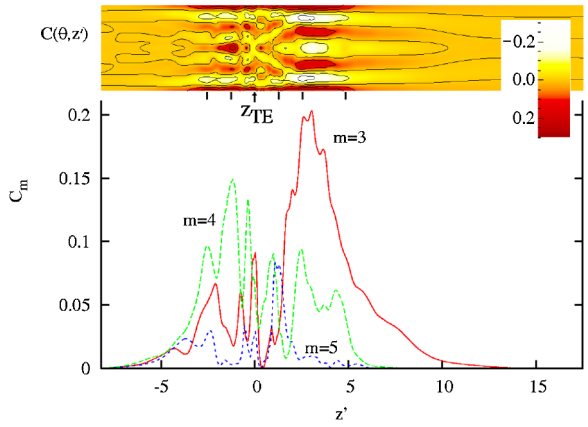

FIG. 3 (color online). Instantaneous correlations for the puff snapshot of Fig. 2(c) at positions relative to the trailing edge $z' = z - z_{\mathrm{TE}}$. In the upper plot θ goes from 0 to 2π vertically; contour intervals of 0.1. The marks below indicate the positions of the cross sections of Fig. 2(d).

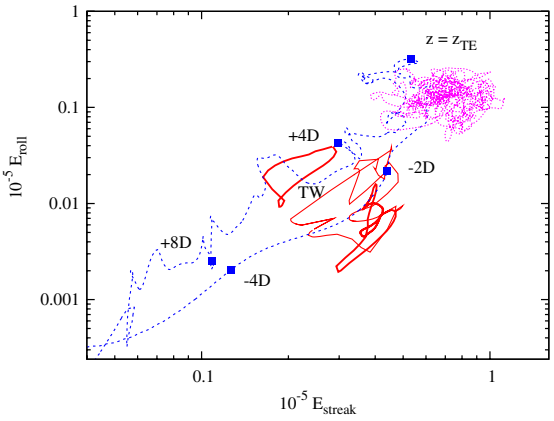

FIG. 5 (color online). Roll and streak energies at different parts of the puff of Fig. 2(c) (Re = 2000). Expanding in Fourier modes m in θ, the total streak and roll energies are defined as $E_{\mathrm{streak}}(z') := \mathrm{Re}^2\pi\sum_{m\neq 0}\int |u'_{mz}|^2 r dr$ and $E_{\mathrm{roll}}(z') := \mathrm{Re}^2\pi\sum_{m\neq 0}\int(|u'_{mr}|^2 + |u'_{m\theta}|^2) r dr$ in units $\rho\nu^2$. Here $\boldsymbol{u}' = (u'_r, u'_\theta, u'_z)$ is the deviation from the laminar profile, for easier comparison with the TWs. Energies for two-, three- and fourfold rotationally symmetric TWs [11] are shown using lower thick, middle thin and upper thick red solid lines, respectively (the closed loops are produced by the finite continuum of TW axial wave numbers which can exist at Re = 2000). The pink short-dotted line "cloud" in the top right hand corner corresponds to a slug at Re = 2800.

formed coherent structures, the magnitudes of streak and roll energies are both consistent with TWs which all have a characteristically small roll-to-streak energy ratio.

At higher Re, the turbulence becomes delocalized as the puffs expand to invade the whole flow. The strongly turbulent region around the trailing edge also lengthens to swallow up the weaker relaminarization zones so that the flow spatially homogenizes. Correlations can then be further averaged over the pipe length $C_m := \langle C_m(z)\rangle_z$ where u'_z is now taken as the deviation from the full-space-and-time-averaged profile. Figure 4 shows a clear trend in which the preferred structures are gradually decreasing in scale from $m = 3$ and 4 streaks at Re = 2000 to $m = 4$ and 5 streak structures at Re = 2800. A typical correlation episode in split puffs at Re = 2400 is shown in Fig. 6 using three snapshots $4D/U$ apart. There are two coherent structures simultaneously present in the $25D$ section shown which translate with phase speeds of $\approx(1 \pm 0.1)U$. As in the puff, however, transient signatures of TWs are found to occur in the less energetic regions of puff turbulence.

At larger Reynolds numbers, Re $\gtrsim$ 2800, the turbulent intensity in slug turbulence is uniformly high everywhere, being comparable to that at the trailing edge of a puff (in units of $\rho\nu^2$ at each cross-section), and is never as low as that of the TWs (see Fig. 5). Although fast streak structures are still observed, they are of too high energy to be associated with known TWs. The cross-section shown in Fig. 2(f) ($C_5 > 0.1$) from a slug is typical, where a large and strongly retarded central core dominates, with only narrow fingers extending towards the gaps between the intense fast streaks at the wall [19]. This retarded core feature of the coherent structures found at Re $\gtrsim$ 2800 can now be appreciated as a significant problem in previous qualitative comparisons between slug cross sections and known TWs [14,15]. It is more likely that these coherent structures instead point to the existence of other types of exact, more highly nonlinear solutions.

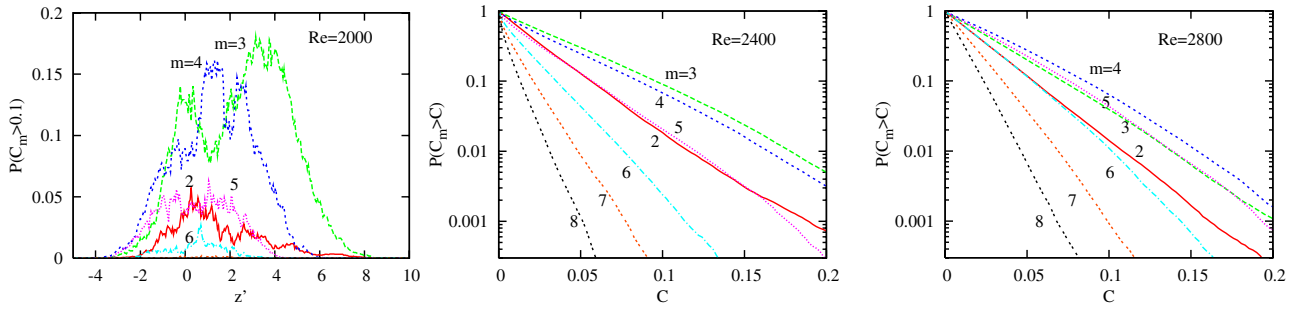

FIG. 4 (color online). Probability at different parts of a puff of a good correlation $C_m(z') \gtrsim 0.1$ (see Fig. 3) at Re = 2000 (left). Probability of a correlation $C_m > C$ at any given point in the flow for Re = 2400 (middle) and 2800 (right).

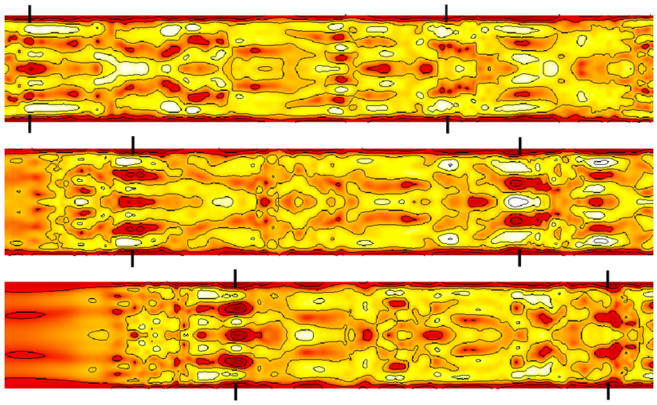

FIG. 6 (color online). Correlations in inhomogeneous turbulence (Re = 2400) at time intervals of $4D/U$, in a fixed window of $25D$ of the domain. The middle snapshot corresponds to that of Fig. 2(b). Same scales as Fig. 3. The black lines mark positions of waves at the different times indicating the translation of the TWs. The phase speeds appear $\approx (1 \pm 0.1)U$.

Our results suggest that the known TWs populate an intermediate region of phase space between the laminar and fully turbulent phases, rather than the turbulent part of phase space itself. The dynamical importance of the TWs is therefore in the transition-to-turbulence process where the fate of an initial disturbance is of concern rather than in characterizing the established turbulent state. The puff provides a simple illustrative example of this picture of TWs sitting between the laminar and turbulent states. At Re = 2000, a puff travels at only $\approx$90% of the bulk velocity so, on average, fluid passes through it. Far upstream ($t \to -\infty$), the fluid ''trajectory'' starts at the origin (laminar state), passes through the TW region of phase space as t increases, to reach the fully turbulent region near the trailing edge. On leaving here as time increases, it passes back through the TW region to the origin as it relaminarizes far downstream ($t \to +\infty$). Consequently, TWs are only visited just up- and downstream of the trailing edge: Fig. 5 is a good 2D representation of this process (where z plays the role of t and a phase space norm based on the streak and roll energies is implied).

Our results confirm emerging evidence that lower branch TWs lie strictly between the laminar and turbulent states in phase space [10,20–22]. However, the fact that upper branches of the known TWs also have too low energy to be associated with the turbulent part of phase space is a surprise. It is quite plausible that the coherent structures observed so far for Re $\gtrsim$ 2800 and characterized by an outer ring of fast streaks together with a strongly decelerated core represent a more-energetic branch of TWs which *is* embedded in the turbulent attractor. The fact that their roll-to-streak energy ratio is so much larger than for currently known TWs suggests that they may have a different sustaining mechanism.

We thank Jorge Peixinho and Tom Mullin for many valuable discussions, and particularly Tom for challenging us to produce Fig. 2. This research was funded by the EPSRC under Grant No. GR/S76144/01.

*A.Willis@bris.ac.uk
†R.R.Kerswell@bris.ac.uk

[1] I. J. Wygnanski and F. H. Champagne, J. Fluid Mech. **59**, 281 (1973).
[2] J. Peixinho and T. Mullin, J. Fluid Mech. **582**, 169 (2007).
[3] S. Bottin and H. Chate, Eur. Phys. J. B **6**, 143 (1998).
[4] M. Nagata, J. Fluid Mech. **217**, 519 (1990).
[5] F. Waleffe, Phys. Rev. Lett. **81**, 4140 (1998).
[6] F. Waleffe, J. Fluid Mech. **435**, 93 (2001).
[7] H. Faisst and B. Eckhardt, Phys. Rev. Lett. **91**, 224502 (2003).
[8] H. Wedin and R. R. Kerswell, J. Fluid Mech. **508**, 333 (2004).
[9] C. C. T. Pringle and R. R. Kerswell, Phys. Rev. Lett. **99**, 074502 (2007).
[10] R. R. Kerswell and O. R. Tutty, J. Fluid Mech. **584**, 69 (2007).
[11] R. R. Kerswell, Nonlinearity **18**, R17 (2005).
[12] B. Eckhardt, T. M. Schneider, B. Hof, and J. Westerweel, Annu. Rev. Fluid Mech. **39**, 447 (2007).
[13] T. M. Schneider, B. Eckhardt, and J. Vollmer, Phys. Rev. E **75**, 066313 (2007).
[14] B. Hof *et al.*, Science **305**, 1594 (2004).
[15] B. Hof, C. W. H. van Doorne, J. Westerweel, and F. T. M. Nieuwstadt, Phys. Rev. Lett. **95**, 214502 (2005).
[16] A. P. Willis and R. R. Kerswell, Phys. Rev. Lett. **98**, 014501 (2007).
[17] The position of an e^{-1} drop from the peak to background value in u_z on the axis was used to set the location of the trailing edge, z_{TE}, where u_z was smoothed over $\pm 1D$ to avoid jumps when monitoring z_{TE} caused by the incursion of vortices shed upstream.
[18] J. Peixinho and T. Mullin, Phys. Rev. Lett. **96**, 094501 (2006).
[19] Plotting the flow relative to a different profile may change Fig. 2(f) slightly, and may reduce the relative streak energy of the perturbation, but cannot resolve the disparity in roll energies.
[20] T. Itano and S. Toh, J. Phys. Soc. Jpn. **70**, 703 (2001).
[21] J. Wang, J. F. Gibson, and F. Waleffe, Phys. Rev. Lett. **98**, 204501 (2007).
[22] Y. Duguet, A. P. Willis, and R. R. Kerswell, arXiv.org/abs/0711.2175 (to be published).
[23] V. G. Priymak and T. Miyazaki, Phys. Fluids **16**, 4221 (2004).